ChemComm

Accepted Manuscript

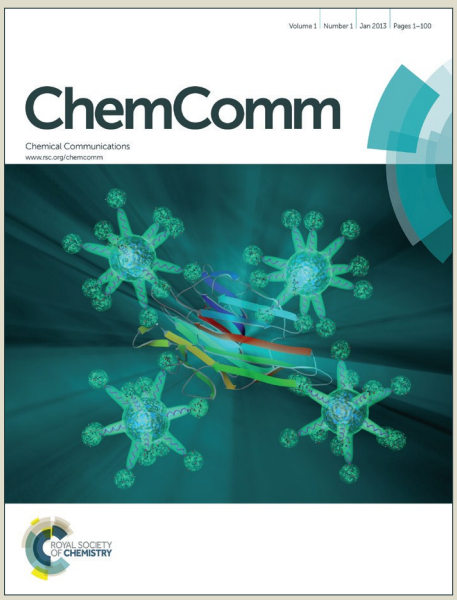

ROYAL SOCIETY OF CHEMISTRY

www.rsc.org/chemcomm

Journal Name

COMMUNICATION

Novel Preparation of Core-shell Electrode Materials via Evaporation-Induced Self-Assembly of Nanoparticles for Advanced Li-Ion Batteries

Zhiqiang Xie[a], Sarah Ellis[a], Wangwang Xu[a], Dara Dye[a], Jianqing Zhao*[a] and Ying Wang*[a]

Received 00th January 20xx,
Accepted 00th January 20xx

DOI: 10.1039/x0xx00000x

www.rsc.org/

We report, for the first time, simple and novel synthesis of a Li-rich layered-spinel core-shell heterostructure (L@S core-shell) via evaporation-induced self-assembly (EISA) of Ni-doped $Li_4Mn_5O_{12}$ nanoparticles ($Li_4Mn_{4.5}Ni_{0.5}O_{12}$) onto the surface of layered $Li[Li_{0.2}Mn_{0.54}Ni_{0.13}Co_{0.13}]O_2$ (LMNCO) without using any surfactant during the coating process. The resultant L@S core-shell as cathode in lithium ion batteries demonstrates significantly improved specific capacity, cycling performance and rate capability compared to pristine LMNCO.

The main drawbacks of commercial $LiCoO_2$ cathode material such as limited delivery capacity, toxicity as well as high cost have hindered its application in plug-in hybrid electric vehicles (PHEV) or electric vehicles (EV).[1,2] In this regard, Li-rich layered oxides have attracted extensive attention due to its high specific capacity of ~250 mAh/g when cycled over a broad voltage range between 2.0 and 4.8 V verses Li/Li^+ and other advantages such as environmental benignity, safety and relatively low cost.[3,4] Among Li-rich layered oxides, $Li[Li_{0.2}Mn_{0.54}Ni_{0.13}Co_{0.13}]O_2$, a solid solution in a two component notation as $0.5Li_2MnO_3{\cdot}0.5LiMn_{1/3}Ni_{1/3}Co_{1/3}O_2$ (hereafter marked as LMNCO), has attracted extensive attention due to its extremely high theoretical capacity of 321 mAh/g, better cycling stability and rate capability than other Li-rich analogs. Unfortunately, these materials still suffer from unsatisfactory cycling stability and intrinsically poor rate capability.[3,4,5] Moreover, it has been reported that Li-rich layered oxides suffer from surface vulnerability at high voltage and erosion from electrolytes.[6,7,8,9] In order to address these challenges, many efforts have been devoted to improving the structural and surface stabilities by using a simple surface modification strategy. Up to now, various metal oxides (Al_2O_3,[10] CeO_2[11] etc.), fluorides and phosphates,[12-14] as well as some other Li-ion conducting $LiNiPO_4$,[15,16] $LiAlO_2$[17] and Li_2ZrO_3[18] have been applied to stabilize the surface structure of Li-rich layered oxides and suppress side-reactions between the electrode and electrolyte, thereby leading to improved cycling performance and thermal stability. However, such coating materials are either poor electronic or ionic conductors and generally are not electrochemically active, thereby leading to limited improvement in electrochemical performance of Li-rich layered oxides.

Recently, lithium manganese oxides (LMO) based spinel cathodes have attracted intensive attention due to its high rate capability resulted from its efficient 3D Li^+ diffusion channels.[19,20] Among them, spinel $Li_{1+x}Mn_2O_4$ has been studied as the coating material to overcome the above-mentioned drawbacks of Li-rich layered oxide material.[21] In this design of layered-spinel core-shell heterostructure, the spinel coating with efficient 3D Li-ion transport channels was expected to stabilize the layered bulk upon high-voltage cycling and rapidly transport Li ions between the layered bulk and electrolyte, leading to improvements in both cycling stability and rate capability of Li-rich layered oxide cathode. However, preparation of core-shell heterostructures reported in literature required complex procedures and precise control of reaction conditions such as pH and concentration of the solutions, which poses challenges for large-scale production for high-energy high-power LIBs.[22] In addition, the spinel $Li_{1+x}Mn_2O_4$ has been reported to have an unsatisfactory cycling stability due to Jahn-Teller distortion and manganese dissolution through a disproportionation reaction. [23,24]

To improve electrochemical property of conventional spinel $Li_{1+x}Mn_2O_4$, it is found in our recent work that Ni-doped spinel $Li_4Mn_5O_{12}$ ($Li_4Mn_{4.5}Ni_{0.5}O_{12}$) can be charged to around 5.0 V and show remarkable high-voltage cycling stability at room temperature.[25] In addition, its 3D Li^+ ion diffusion pathways ensure its excellent rate capability.[26] Therefore, it can be expected to be a promising coating material to replace spinel $Li_{1+x}Mn_2O_4$. Herein, we report a simple and facile one-pot preparation of L@S core-shell

[a] Department of Mechanical & Industrial Engineering, Louisiana State University, Baton Rouge, LA 70803, USA. E-mail: andrewxie1020@gmail.com
* Department of Mechanical & Industrial Engineering, Louisiana State University, Baton Rouge, LA 70803, USA. Prof. Ying Wang, E-mail: ywang@lsu.edu; Fax: +1-225-578-9162; Tel: +1-225-578-8577; Dr. Jianqing Zhao, E-mail: jzhao3@tigers.lsu.edu; Fax: +1-225-578-9162; Tel: +1-225-329-3539

Electronic Supplementary Information (ESI) available: Experimental details, SEM image of Ni-doped spinel $Li_4Mn_{4.5}Ni_{0.5}O_{12}$, CV curves of pristine LMNCO and spinel $Li_4Mn_{4.5}Ni_{0.5}O_{12}$. See DOI: 10.1039/x0xx00000x

structure (Li-rich layered-spinel core-shell heterostructure) via evaporation-induced self-assembly (EISA) of ultrafine $Li_4Mn_{4.5}Ni_{0.5}O_{12}$ nanoparticles onto the surface of Li-rich layered $Li[Li_{0.2}Mn_{0.54}Ni_{0.13}Co_{0.13}]O_2$ (LMNCO) without using any surfactant during the coating process. In this study, we also introduce a simple route to prepare ultrafine $Li_4Mn_{4.5}Ni_{0.5}O_{12}$ nanoparticles (5~20 nm) from the spinel $Li_4Mn_{4.5}Ni_{0.5}O_{12}$ bulk by the so-called sonofragmentation. Sonofragmentaion is a well-known one-step process to directly produce nanoparticles from large-grained powders.[27, 28] It has been reported that even intrinsically strong carbon nanotubes can be fragmented by sonication.[29] As a result, the as-prepared L@S core-shell material demonstrates significantly improved specific capacity, cycling performance and rate capability for application as cathode in new-generation LIBs compared to pristine LMNCO. Due to the structural and functional versatility of nanoparticles, the synthetic approach reported in this work can be generalized to other materials to form novel core-shell structures, for the application in LIBs or other fields.

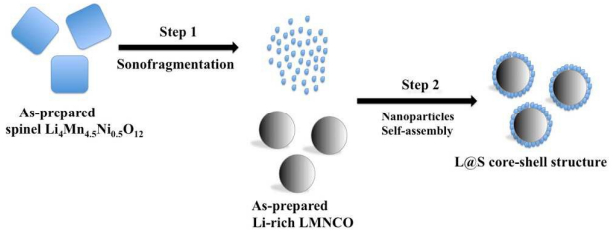

Fig. 1. Schematic illustration of facile preparation of L@S core-shell heterostructure.

Fig.1 presents a schematic illustrating the facile synthesis procedure of L@S core-shell heterostructure via EISA, which is different from existing methods such as "dip and dry"[21] or co-precipitation.[22] Briefly, simple top-down preparation of spinel $Li_4Mn_{4.5}Ni_{0.5}O_{12}$ nanoparticles is introduced by applying ultrasonication to larger $Li_4Mn_{4.5}Ni_{0.5}O_{12}$ particles in ethanol for two hours. The large-sized $Li_4Mn_{4.5}Ni_{0.5}O_{12}$ particles are broken into smaller nanoparticles due to mechanical energy of ultrasonic wave. Afterwards, as described in the experimental part, the resultant suspension of $Li_4Mn_{4.5}Ni_{0.5}O_{12}$ ultrafine nanoparticles in ethanol are mixed with $Li[Li_{0.2}Mn_{0.54}Ni_{0.13}Co_{0.13}]O_2$ suspension in ethanol, followed by continuously stirring at 80°C until the solvent is completely evaporated. In this step, ultrafine nanoparticles of $Li_4Mn_{4.5}Ni_{0.5}O_{12}$ tend to self-assembly on the surface of large-sized $Li[Li_{0.2}Mn_{0.54}Ni_{0.13}Co_{0.13}]O_2$ particles in order to drastically reduce surface energy. Finally, after post-annealing at 500°C for 3 hours, L@S core-shell heterostructure is successfully obtained.

The as-prepared spinel $Li_4Mn_{4.5}Ni_{0.5}O_{12}$ particles are characterized by both scanning electron microscopy (SEM) and transmission electron microscopy (TEM). The SEM image of $Li_4Mn_{4.5}Ni_{0.5}O_{12}$ particles before sonofragmentation in Figure S1 shows numerous highly-crystalline nanoparticles with smooth surfaces. Fig. 2a and b display TEM and high-resolution TEM (HRTEM) images of spinel $Li_4Mn_{4.5}Ni_{0.5}O_{12}$ powders before and after sonofragmentation, respectively. Figure 2a reveals the average size of primary $Li_4Mn_{4.5}Ni_{0.5}O_{12}$ particles is ~500 nm. Interestingly, it is found in Figure 2b and c that sonication can effectively reduce the particle size of $Li_4Mn_{4.5}Ni_{0.5}O_{12}$ powders into nanoscale (5~20 nm). The lattice fringes of each nanoparticle in Fig.2c are clearly observed. The zoom-in view of two regions in green rectangles in Fig. 2b is displayed in Fig. 2c and d. The lattice fringes of the $Li_4Mn_{4.5}Ni_{0.5}O_{12}$ surface coating can be readily indexed to the planes of (222), (400) and (220), respectively, suggesting the efficient preparation of ultrafine monocrystalline nanoparticles by using the sonication treatment. This approach demonstrates a promising way to produce various inorganic nanoparticles and will find wide potential applications in many fields such as nano-scale electronic devices.

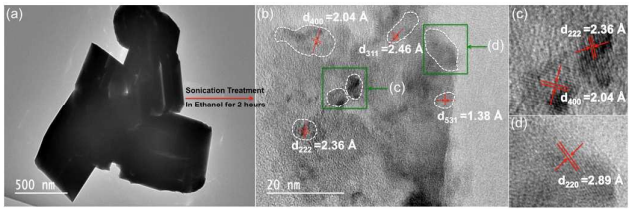

Fig. 2. (a) TEM bright field images of spinel $Li_4Mn_{4.5}Ni_{0.5}O_{12}$ particles before sonofragmentation, (b) HRTEM image of $Li_4Mn_{4.5}Ni_{0.5}O_{12}$ after sonofragmentation, with (c) and (d) showing zoom-in view of two regions in the green rectangles in (b).

As revealed in the SEM image of pristine layered LMNCO in Fig. 3a, the sample is composed of nanoparticles (~200 nm) with smooth surface, indicating their highly crystalline nature. It is noted that L@S core-shell sample looks very similar to LMNCO particles under SEM since the ultrathin coating cannot be detected by SEM. Therefore, TEM is used to examine morphology of the core-shell structure as shown in Fig. 3c and d. Crystal structures of the as-prepared pristine layered LMNCO, spinel $Li_4Mn_{4.5}Ni_{0.5}O_{12}$ and L@S core-shell samples are further identified using powder X-ray diffraction (XRD) as shown in Fig. 3b. The main peaks from the $Li_4Mn_{4.5}Ni_{0.5}O_{12}$ sample can be readily indexed to $Li_4Mn_5O_{12}$ with spinel phase of face-centered cubic structure (ICDD: 46-0810). A secondary phase of monoclinic Li_2MnO_3 with C2/m symmetry (ICDD: 84-1634) is evidenced as well, which might be ascribed to decomposition of $Li_4Mn_5O_{12}$ spinel phase during post-heat treatment at 900°C.[25] The strong peaks from both pristine LMNCO and L@S core-shell heterostructure samples can be indexed as a layered α-$NaFeO_2$ structural type with space group R3m symmetry and some weak superstructure reflections (marked as * in Fig. 3b) can be ascribed to monoclinic phase Li_2MnO_3. Compared to XRD patterns of pristine LMNCO and spinel $Li_4Mn_{4.5}Ni_{0.5}O_{12}$, the XRD pattern from the L@S core-shell heterostructure sample combines with the patterns of both layered structure and cubic spinel structure with weak shoulder peaks assigned to the spinel coating as pointed by the arrows in Fig. 3b.

High-resolution TEM (HRTEM) is used to examine L@S core-shell sample to further identify its surface structure. As observed in Fig. 3c, the bulk layered structure of pristine LMNCO is well-preserved in the L@S core-shell structure, displaying lattice fringes with an interplanar spacing of ca. 4.73 Å. It can also be seen that a homogeneous outer layer is uniformly coated on the surface of layerd LMNCO bulk. The enlarged view in Fig. 3d reveals a crystalline outer layer with lattice fringes showing an interplanar spacing of ca. 1.38 Å, which do not belong to the layered structure but are consistent with the (531) plane of the cubic spinel (Fd-3m), confirming that the outer layer is the spinel coating. Therefore, it can be concluded that novel L@S core-shell structure can be facilely

synthesized via evaporation-induced self-assembly of nanoparticles, which opens new route for achieving various core-shell structures for different applications.

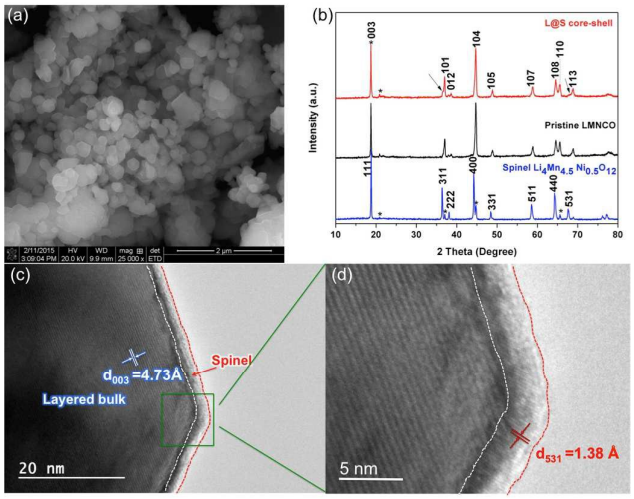

Fig. 3. (a) SEM image of pristine layered LMNCO, (b) Powder XRD patterns of spinel $Li_4Mn_{4.5}Ni_{0.5}O_{12}$, pristine layered LMNCO, L@S core-shell heterostructured powders, (c) HRTEM images of L@S core-shell sample and (d) zoom-in view of the surface of L@S core-shell in the green rectangle in (c).

Fig. 4a and b compares initial three charge/discharge curves of pristine LMNCO and L@S core-shell heterostructured cathodes when cycled between 2.0 and 4.99 V *vs*. Li/Li^+ at 25 mA/g (~0.1 *C*). It is found that L@S core-shell heterostructured cathode is capable of providing a discharge capacity of ~272 mAh/g after three cycles, which is higher than pristine LMNCO that delivers a discharge capacity of ~248 mAh/g. Compared to the discharge plot of pristine LMNCO, two newly-formed plateaus at around 4.7 and 2.7 V are observed for L@S core-shell heterostructured sample, which is associated with the coating of spinel $Li_4Mn_{4.5}Ni_{0.5}O_{12}$.[25, 26] Therefore, lithium ions can be intercalated into the spinel coating at around 4.7 and 2.7 V (marked by arrows) during the discharge process, thereby leading to higher discharge capacities of L@S core-shell structure.

In order to compare cycling stability of L@S core-shell and pristine LMNCO cathodes, both samples are cycled at 0.1 and 0.5 C in the wide high-voltage range between 2.0 – 4.99 V *vs*. Li/Li^+, respectively, as shown in Fig. 4c and d. As observed in Fig. 4 c, pristine LMNCO delivers a maximal capacity of ~258 mAh/g and maintains ~233 mAh/g after 60 cycles at 0.1 *C*. In contrast, L@S core-shell cathode delivers a maximal capacity of ~ 286 mAh/g and retains 273 mAh/g after 60 cycles exhibiting a higher capacity retention of 95.4 % than that of the pristine LMNCO (90.3%). Fig. 4d compares cycling performances of the two samples at a higher rate of 0.5 *C*. In this test, L@S core-shell delivers a maximal capacity of ~ 183 mAh/g and retains ~ 153 mAh/g after 100 cycles, which is much higher than that of pristine LMNCO giving ~125 mAh/g after 100 cycles. The improvement in cycling performance and specific capacity herein can be ascribed to the stabilizing effect of thin spinel phase coating, which not only helps to reduce the erosion from electrolyte under high voltage but also restrain the bulk LMNCO active-mass loss during long cycling.

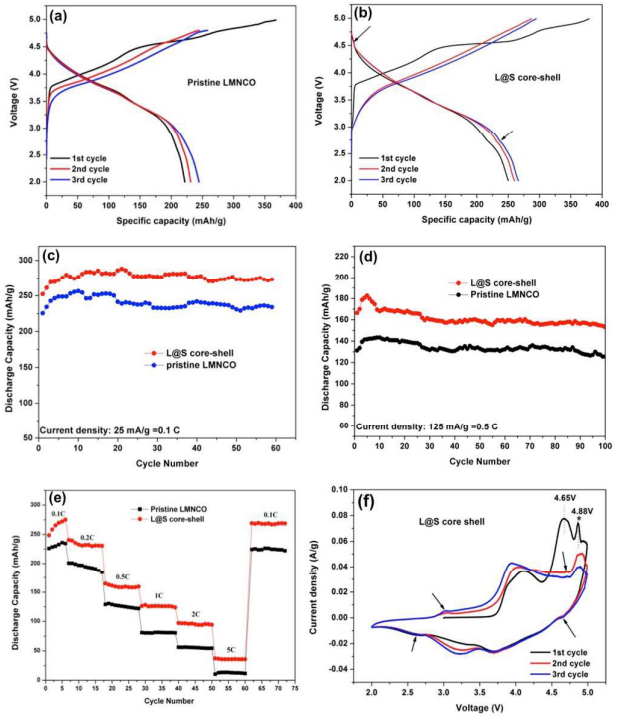

Fig. 4. Initial three charge/discharge curves of (a) pristine layered LMNCO, (b) L@S core-shell heterostructured cathodes when cycled between 2.0 - 4.99 V *vs*. Li/Li^+ at a specific current of 25 mA/g (0.1*C*). (c) and (d): Cycling performances of pristine LMNCO and L@ core-shell cathodes at 0.1 and 0.5 *C*, respectively. (e) Rate performances of pristine LMNCO and L@S core-shell cathodes at various charge/discharge rates. (f) Cyclic voltammograms of L@S core-shell cathode in the first three cycles at a scan rate of 0.1 mV/s in a voltage range of 2.0 - 4.99 V *vs*. Li/Li^+.

Fig. 4e summarizes rate performances of pristine LMNCO and L@S cathodes at various charge/discharge rates, namely 0.1 *C*, 0.2 *C*, 0.5 *C*, 1 *C*, 2 *C* and 5 *C* at 2.0 – 4.99 V *vs*. Li/Li^+. It is found that pristine LMNCO shows a poor rate capability, with almost no discharge capacity at 5 *C* though a good recovery to ~225 mAh/g when cycled back to 0.1 *C*. On the contrary, L@S core-shell sample delivers initial discharge capacities of 126 mAh/g, 97 mAh/g and 37 mAh/g at 1 *C*, 2 *C* and 5 *C*, respectively; when cycled back to 0.1 *C* from 5 *C*, its discharge capacity reaches as high as 269 mAh/g, demonstrating an outstanding electrochemical reversibility. Such enhanced rate performance is resulted from the following factors. First, the spinel coating with excellent structural stability can effectively stabilize the surface structure of LMNCO core, thereby reducing the erosion from the electrolyte and the bulk active-mass lose. Second, the spinel coating facilitates fast Li ions diffusion from the electrolyte to the layered LMNCO core. In addition, due to structural compatibility between the layered LMNCO and spinel phase coating, L@S is expected to have high structural stability. It is also noted that the L@S core-shell cathode needs more charge-discharge cycles to reach its maximum capacity at 0.1 *C* than pristine LMNCO cathode. The reason for this difference can be attributed to the relatively uniform spinel $Li_4Mn_{4.5}Ni_{0.5}O_{12}$ coating at the outer surface of the LMNCO core, which leads to the gradual electrochemical activation of the Li_2MnO_3 component in LMNCO

core during the initial several cycles. As a result, L@S core-shell composite cathode needs more electrochemical cycles to reach its maximum capacity in comparison with the pristine LMNCO.

Cyclic voltammetric (CV) measurements are then carried out to further explore electrochemical characteristics of the core, shell, and core-shell materials. Fig. S2 presents the first CV three cycles of pristine LMNCO and spinel $Li_4Mn_{4.5}Ni_{0.5}O_{12}$, respectively, at a scan rate of 0.1 mV/s in the voltage range of 2.0 - 4.99 V. As for the CV curve of pristine LMNCO (Fig. S2a), the first pair of redox peaks at 4.16/3.63 V in the first electrochemical cycle corresponds to the redox reactions of Ni^{2+}/Ni^{4+} followed by Co^{3+}/Co^{4+}, while Mn still remains as tetravalent in $LiMn_{1/3}Ni_{1/3}Co_{1/3}O_2$ structure.[30,31] The anodic peak at 4.67 V is associated with decomposition of Li_2MnO_3 to Li_2O and Li-active MnO_2, the unavoidable decomposition of electrolyte and formation of solid electrolyte interphase (SEI) at such a high potential above 4.5 V.[32] Such an electrochemical activation process of Li_2MnO_3 would result in high capacity of LMNCO via simultaneously losing oxygen irreversibly as Li_2O and MnO_2. Therefore, the cathodic peak at ~3.0 V becomes apparent after charging to 4.99 V and can be attributed to the redox reaction of Mn^{3+}/Mn^{4+} that may take place in the electrochemical reaction after the Li_2MnO_3 component is electrochemically activated. It is also found that the anodic peak at 4.67 V in the first CV curve disappears in subsequent CV cycles. Fig. S2b displays a typical CV curve of spinel $Li_4Mn_{4.5}Ni_{0.5}O_{12}$. It is clearly observed that the 2nd and 3rd curves of spinel $Li_4Mn_{4.5}Ni_{0.5}O_{12}$ are almost identical, indicating outstanding electrochemical reversibility and structural stability during cycling over a wide voltage range between 2.0 and 4.99 V *vs*. Li/Li^+, which is expected to be a promising surface coating for pristine LMNCO. In the CV curves of LMNCO coated with spinel $Li_4Mn_{4.5}Ni_{0.5}O_{12}$ (L@S core-shell) as shown in Fig. 4f, it is found that the L@S core-shell cathode shows a slightly better electrochemical reversibility than pristine LMNCO. The redox peaks at 4.16/3.63 V are associated with oxidation of Co^{3+}/Co^{4+} redox only from LMNCO core and Ni^{2+}/Ni^{4+} redox from both LMNCO core and spinel $Li_4Mn_{4.5}Ni_{0.5}O_{12}$ shell. Interestingly, the above redox peaks from L@S core-shell show higher corresponding current density than that of pristine LMNCO, probably attributed to the thin spinel coating that reduces the erosion from electrolyte and transition-metal ion dissolution. It is also noted that some peaks (pointed by arrows in the Fig.4f) and another extra peak at 4.88 V can be ascribed to the spinel phase coating, confirming the L@S core-shell heterostructure, which is consistent with the XRD and TEM results.

In conclusion, we report simple and novel synthesis of L@S core-shell structured electrode material via facile evaporation-induced self-assembly (EISA) of ultrafine crystalline $Li_4Mn_{4.5}Ni_{0.5}O_{12}$ nanoparticles on the surface of Li-rich layered $Li[Li_{0.2}Mn_{0.54}Ni_{0.13}Co_{0.13}]O_2$ particles. This L@S core-shell cathode material demonstrates significantly improved specific capacity, cycling performance and rate capability compared to pristine Li-rich layered cathode. Due to structural and functional versatility of nanoparticles, our study provides new insights into preparation of various core-shell structures via EISA of nanoparticles for applications in LIBs or other energy-related fields.

This work is supported by the Research Enhancement Award (REA) and the Research Awards Program (RAP) sponsored by LaSPACE.

Notes and references

[1] J. B. Goodenough and Y. Kim, *Chem. Mat.,* 2010, **22**, 587.
[2] M. Armand and J. M. Tarascon, *Nature*., 2008, **451**, 652.
[3] B. Xu, C. R. Fell, M. Chi, Y. S. Meng, *Energy Environ. Sci*., 2011, **4**, 2223.
[4] M. Gu, A. Genc, I. Belharouak, D. Wang, K. Amine, S. Thevuthasan, D. R. Baer, J. G. Zhang, N. D. Browning, J. Liu and C. Wang, *Chem. Mater*., 2013, **25**, 2319.
[5] H. Yu and H. Zhou, *J. Phys. Chem. Lett*., 2013, **4**, 1268.
[6] D. Wang, I. Belharouak, G. Zhou and K. Amine, *Adv. Funct. Mater*., 2012, **23**, 1070.
[7] L. Chen, Y. F. Su, S. Chen, N. Li, L. Y. Bao, W. K. Li, Z. Wang, M. Wang and F. Wu, *Adv. Mater*., 2014, **26**, 6756.
[8] H. Liu, C. Y. Du, G. P. Yin, B. Song, P. J. Zuo, X. Q. Cheng, Y. L. Ma and Y. Z. Gao, *J. Mater. Chem. A*., 2014, **2**, 15640.
[9] A. R. Armstrong, M. Holzapfel, P. Novak, C. S. Johnson, S. H. Kang, M. M. Thackeray and P. G. Bruce, *J. Am. Chem. Soc*., 2006, **128**, 8694.
[10] G. S. Zou, X. K. Yang, X. Y. Wang, L. Ge, H. B. Shu, Y. S. Bai, C. Wu, H. P. Guo, L. Hu, X. Yi, B. W. Ju, H. Hu, D. Wang, R. Z. Yu, *J. Solid State Electrochem*., 2014, **18**, 1789.
[11] W. Yuan, H. Z. Zhang, Q. Liu, G. R. Li, X. P. Gao, *Electrochim. Acta*, 2014, 135, 199.
[12] Y. K. Sun, M. J. Lee, C. S. Yoon, J. Hassoun, K. Amine and B. Scrosati, *Adv. Mater*., 2012, **24**, 1192.
[13] M. S. Park, J. W. Lee, W. Choi, D. Im, S. G. Doo and K. S. Park, *J. Mater. Chem*., 2010, **20**, 7208.
[14] Q. Wang, J. Liu, A. V. Murugan and A. Manthiram, *J. Mater. Chem*., 2009, **19**, 4965.
[15] S. H. Kang and M. M. Thackeray, *Electrochem. Commun*., 2009, **11**, 748.
[16] J. R. Croy, M. Balasubramanian, D. Kim, S. H. Kang and M. M. Thackeray. *Chem. Mat*., 2011, **23**, 5415.
[17] H. S. Kim, Y. Kim, S. I. Kim, and S. W. Martin, *J. Power Sources*., 2006, **161**, 623.
[18] X. P. Zhang, S. W. Sun, Q. Wu, N. Wan, D. Pan and Y. Bai, *J. Power Sources*., 2015, **282**, 378.
[19] S. Ivanova, E. Zhecheva, D. Nihtianova, M. Mladenov and R. Stoyanova, *J. Alloys Compd*., 2013, **561**, 252.
[20] J. Cao, J. Xie, G. Cao, T. Zhu, X. Zhao and S. Zhang, *Electrochim. Acta*., 2013, **111**, 447.
[21] F. Wu, N. Li, Y. F. Su, L. J. Zhang, L. Y. Bao, J. Wang, L. Chen, Y. Zheng, L. Q. Dai, J. Y. Peng, and S. Chen, *Nano Lett*., 2014, **14**, 3550.
[22] Q. B. Xia, X. F. Zhao, M. Q. Xu, Z. P. Ding, J. T. Liu, L. B. Chen, D. G. Ivey and W. F. Wei, *J. Mater. Chem. A*., 2015, **3**, 3995.
[23] K. S. Lee, H. J. Bang, S. T. Myung, J. Prakash, K. Amine and Y. K. Sun, *J. Power Sources*., 2007, **174**, 726.
[24] M. Hirayama, H. Ido, K. Kim, W. Cho, K. Tamura, J. Mizuki and R. Kanno, *J. Am. Chem. Soc*., 2010, **132**, 15268.
[25] Z. Q. Xie, H. Eikhuemelo, J. Q. Zhao, C. Cain, W. W. Xu and Y. Wang, *J. Electrochem. Soc*., 2015, **162**, A1523. .
[26] J. Q. Zhao, S. Ellis, Z. Q. Xie and Y. Wang, *ChemElectroChem*., in press.
[27] K. A. Kusters, S. E. Pratsinisap, S. G. Thorna and D. M. Smith, *Powder Technol*., 1994, **80**, 253.
[28] M. D. Kass, *Mater. Lett*., 2000, **42**, 246.
[29] Y. Y. Huang, T. P. J. Knowles and E. M. Terentjev, *Adv. Mater*., 2009, **21**, 3945.
[30] T. Zhao, S. Chen, L. Li, X. Zhang, R. Chen, I. Belharouak, F. Wu and K. Amine,
J. Power Sources., 2013, **228**, 206.
[31] T. H. Cho, Y. Shiosaki and H. Noguchi, *J. Power Sources*., 2006, **159**,1322.
[32] S. K. Martha, J. Nanda, G. M. Veith and N. J. Dudney, *J. Power Sources*., 2012, **199**, 220.